The EMBO Journal (2013) 32, 60–71
www.embojournal.org

OPEN ACCESS TRANSPARENT PROCESS

THE EMBO JOURNAL

Dissecting the mechanisms of Notch induced hyperplasia

Alexandre Djiane[1], Alena Krejci[2], Frédéric Bernard, Silvie Fexova, Katherine Millen and Sarah J Bray*

Department of Physiology, Development and Neuroscience, University of Cambridge, Cambridge, UK

The outcome of the Notch pathway on proliferation depends on cellular context, being growth promotion in some, including several cancers, and growth inhibition in others. Such disparate outcomes are evident in *Drosophila* wing discs, where Notch overactivation causes hyperplasia despite having localized inhibitory effects on proliferation. To understand the underlying mechanisms, we have used genomic strategies to identify the Notch-CSL target genes directly activated during wing disc hyperplasia. Among them were genes involved in both autonomous and non-autonomous regulation of proliferation, growth and cell death, providing molecular explanations for many characteristics of Notch induced wing disc hyperplasia previously reported. The Notch targets exhibit different response patterns, which are shaped by both positive and negative feed-forward regulation between the Notch targets themselves. We propose, therefore, that both the characteristics of the direct Notch targets and their cross-regulatory relationships are important in coordinating the pattern of hyperplasia.

The EMBO Journal (2013) **32,** 60–71. doi:10.1038/emboj.2012.326; Published online 11 December 2012
Subject Categories: signal transduction; genomic & computational biology
Keywords: chromatin immunoprecipitation; *Drosophila*; gene expression; Notch; proliferation

Introduction

The highly conserved Notch cell-cell signalling pathway controls a wide variety of cell fate decisions and governs numerous developmental processes (Bray, 2006). It is also involved in the homeostasis and biology of adult tissues, in particular in the regulation of stem cell lineages (Liu *et al*, 2010). The widespread and versatile roles mean that inappropriate Notch activity can have profound consequences. This is epitomized by its contribution to cancers where, depending on tumour type, Notch can have either an oncogenic or a tumour-suppressor role. Examples of the former are found in several carcinomas such as breast, lung, or cervical cancers, where Notch pathway amplification leads to increased proliferation and tumour progression (Ranganathan *et al*, 2011).

A similar dichotomy is evident in many developmental processes. For example, the Notch pathway is critical for the growth and the patterning of the *Drosophila* imaginal discs, but it exerts different effects on proliferation depending on the territories where it is activated. In the wing imaginal disc, a zone of non-proliferation centred around the dorso-ventral boundary (D/V) is organized by high levels of Notch activity (Herranz *et al*, 2008), which represses *myc* (*diminutive*; *dm*) and *bantam* to modulate the activity of E2F. This is in contrast to some other systems where direct upregulation of *myc* by Notch contributes to tumorigenicity (Klinakis *et al*, 2006; Palomero *et al*, 2006; Sharma *et al*, 2006; Weng *et al*, 2006). Elsewhere in the wing disc moderate levels of Notch activation result in increased cell proliferation and reduced cell death (Baonza and Garcia-Bellido, 2000; Giraldez and Cohen, 2003). Indeed ectopic Notch activity can also cause extreme hyperplasia (Go *et al*, 1998).

In those disc regions where it positively promotes cell proliferation, Notch has effects both in the Notch expressing cells, implying a direct cell-autonomous effect, and also in adjacent cells, implying a relay mechanism (de Celis *et al*, 1996; Go *et al*, 1998; Giraldez and Cohen, 2003). The latter non-autonomous effects can be partly accounted for by Wingless, a member of the Wnt family which mediates aspects of the Notch response (de Celis *et al*, 1996; Giraldez and Cohen, 2003) and which contributes to the regulation of *dm/myc* (Herranz *et al*, 2008). However, even in animals mutant for *wingless* (*wg*), cells adjacent to Notch expressing cells continue to proliferate in many regions arguing that other secreted factors are involved (Giraldez and Cohen, 2003). Furthermore, no clear effectors of cell-cycle regulation have been identified in the wing, although in some leukaemic cells and mouse breast tumour models Notch directly regulates genes involved in the G_1 to S-phase transition, including D-type cyclins (Joshi *et al*, 2009; Ling *et al*, 2010). To date the main intermediary in the wing is thought to be *vestigial* (*vg*), which encodes a nuclear protein regulating wing growth and cell cycle (Kim *et al*, 1996; Zecca and Struhl, 2007). However, not all effects of Notch can be explained by Vg, indicating that there must be additional mechanisms (Go *et al*, 1998; Giraldez and Cohen, 2003).

It is clear therefore that activation of Notch results in complex effects on tissue growth, as epitomized by its diverse effects in wing imaginal discs, but how these disparate outcomes are coordinated is unclear. Transcriptional changes are a direct outcome of Notch pathway activity, and hence provide an important insight into the regulatory mechanisms (Bray, 2006). Upon ligand reception, the Notch receptor is

*Corresponding author. Department of Physiology, Development and Neuroscience, University of Cambridge, Downing Street, Cambridge CB2 3DY, UK. Tel.: +44 1223 765222; Fax: +44 1223 333786; E-mail: sjb32@cam.ac.uk
[1]Present address: Institut de Recherche en Cancérologie de Montpellier, Inserm U896 - Université Montpellier1 - CRLC Val d'Aurelle, Campus Val d'Aurelle, 208 Rue des Apothicaires, F-34298 Montpellier Cedex 5, France
[2]Present address: Faculty of Science and Institute of Entomology, Biology Centre of the Czech Academy of Sciences, University of South Bohemia, Branisovska 31, 370 05 Ceske Budejovice, Czech Republic

Received: 8 October 2012; accepted: 6 November 2012; published online: 11 December 2012

cleaved to release its intracellular domain (Nicd), which binds to the CSL DNA-binding protein (Suppressor of Hairless in *Drosophila*) forming a ternary complex that activates transcription. In the absence of Nicd, CSL proteins are complexed with co-repressors and contribute to the repression of target genes (Bray, 2006; Kopan and Ilagan, 2009). One approach to unravel mechanisms underlying different proliferative responses is thus to identify the target genes that are directly regulated by Notch in circumstances where it elicits hyperplasia, such as in wing imaginal discs.

Taking a genome-wide approach we have characterized the repertoire of genes directly activated by Notch in overproliferating *Drosophila* imaginal wing discs by analysing the transcriptional changes and the sites bound by the CSL transcription factor Suppressor of Hairless [Su(H)]. By integrating these data and by comparing results from two complementary approaches to modulate activity of the pathway, we identify targets that explain how Notch can promote cell proliferation in the wing discs both directly and indirectly. Tests to verify their relevance downstream of Notch for tissue growth and their regulation by Notch uncover contributions of the novel targets. Furthermore, cross-regulatory interactions between some of the direct targets explain how different Notch response domains are generated within the tissue.

Results

Identification of Notch target genes involved in hyperplasia

Ectopic or prolonged Notch activity frequently causes tissue hyperplasia, as exemplified by phenotypes produced when the activated form of Notch (Nicd) is expressed in randomly generated clones throughout the wing disc (Figure 1A). Similar hyperplasia arises when the Notch pathway terminal transcription factor Su(H) is expressed using the *patched-Gal4* driver (*ptc-Gal4*; Figure 1B), despite its more restricted expression and its dual role in repression and activation of Notch targets. These two complementary approaches result in broadly similar phenotypes even though the former involves high level of Notch activation in almost all cells of the wing disc, while the latter drives moderate level of Notch activation in fewer cells that ultimately outcompete wild-type cells. Combining the results provides a powerful way to identify Notch targets involved in hyperplasia that might overcome the caveats of each individually. It could also give insight into genes activated at different levels of Notch activity and to mechanisms of regulation.

To identify the genes acting downstream of Notch, we first compared RNA expression profiles from control and hyperplastic wing discs using expression microarrays (Figure 1A–C). Among 365 differentially expressed genes in Nicd hyperplasia and 460 in Su(H) hyperplasia ($P \leqslant 0.05$), 128 were upregulated in both cell types confirming that there are common changes in the two conditions.

To further distinguish genes directly regulated by Notch activity, we performed chromatin immunoprecipitation (ChIP) to identify regions occupied by Su(H) (Krejcí and Bray, 2007), and hybridized the bound DNA fragments to oligonucleotide tiling arrays covering the *Drosophila* genome. The number of bound regions ('peaks') varied between genotypes with many more detected in Nicd hyperplasia ($2\times$) and in Su(H) hyperplasia ($3\times$) than in control. Although the increased peak number was not unexpected in Su(H) discs (as levels of DNA binding protein are vastly elevated), the increased number of bound regions in Nicd discs was unexpected and suggests that cells have excess of Su(H) that could be recruited into stable complexes by the ectopic Nicd. Of the peaks identified, >850 were detected in both Nicd and Su(H) hyperplastic discs. The majority of these (72%) contained motifs that matched a dictionary of known Su(H) binding motifs (results were similar for all Nicd peaks (63%) and all Su(H) peaks (69%)) and 49% had matches to high affinity motifs. There was also a good correspondence between peaks and the location of characterized Notch responsive wing enhancers (e.g., Ser; Figure 1D). We note that there were many examples of clustered peaks, so that often multiple peaks were associated with a single locus (e.g., *unpaired* [*upd*], *Serrate* [*Ser*]; Figure 1D). However, we did not find any correlation between the number of peaks and the fold change in expression (correlation coefficient of 0.15 for Nicd peaks and of 0.04 for Su(H) peaks).

The data were then integrated to identify which differentially expressed genes were associated with Su(H) occupied regions, so-called assigned peak genes (APG; Figure 1C). This parsimonious approach selected strong candidates for direct Notch target genes in each condition and the overlap revealed 58 genes that were upregulated under both conditions (Figure 1C and E). These therefore represent strongest candidates to mediate hyperplastic growth. In all, 81 additional APG were upregulated in Nicd hyperplasia (Figure 1C; Supplementary Tables 1–6) and 197 in Su(H) hyperplasia (Figure 1C; Supplementary Tables 1–6). We note however that several genes which appear as significant ($P \leqslant 0.05$) in only one condition were also upregulated in the other, but with greater variability between replicates. We have therefore considered all APG (336 in total) in some of the subsequent analyses.

Hierarchical clustering of Nicd and Su(H) APG targets also revealed a group of genes (30) that were strongly upregulated by Nicd but downregulated by Su(H) (Figure 1E). Included were bHLH genes of the *E*(*spl*) complex, well-known Notch targets, as well as *Notch* (*N*), *bigbrain* and *Delta* (*Dl*), Notch pathway components. Despite these differences, the Su(H) binding profile at such loci was similar in both Nicd and Su(H) hyperplastic discs. While some differences between the expression changes may be the consequence of variations between the cell populations that overgrow in the two manipulations, the observation that two target enhancers (*E*(*spl*)*mβ* and *E*(*spl*)*m8*) were downregulated in the cells expressing Su(H) (Supplementary Figure 1H and I) suggests that alternate regulatory mechanisms could also contribute. It has previously been proposed that, by competing with the available Nicd, excess Su(H) can prevent upregulation of some targets (Furriols and Bray, 2000).

Functional characteristics of hyperplasia-associated Notch targets

To distinguish the extent to which Notch induced hyperplasia is achieved indirectly (by regulating cell-fate determinants and/or mitogens) or directly (by acting on cell cycle or proliferation control genes), functional characteristics of the direct Notch targets (APG targets) were analysed using gene ontology (GO) and protein domain annotations (http://david.abcc.ncifcrf.gov/). Importantly, the enriched categories ($P \leqslant 0.05$) included 4 related to cell proliferation, 3 to organ

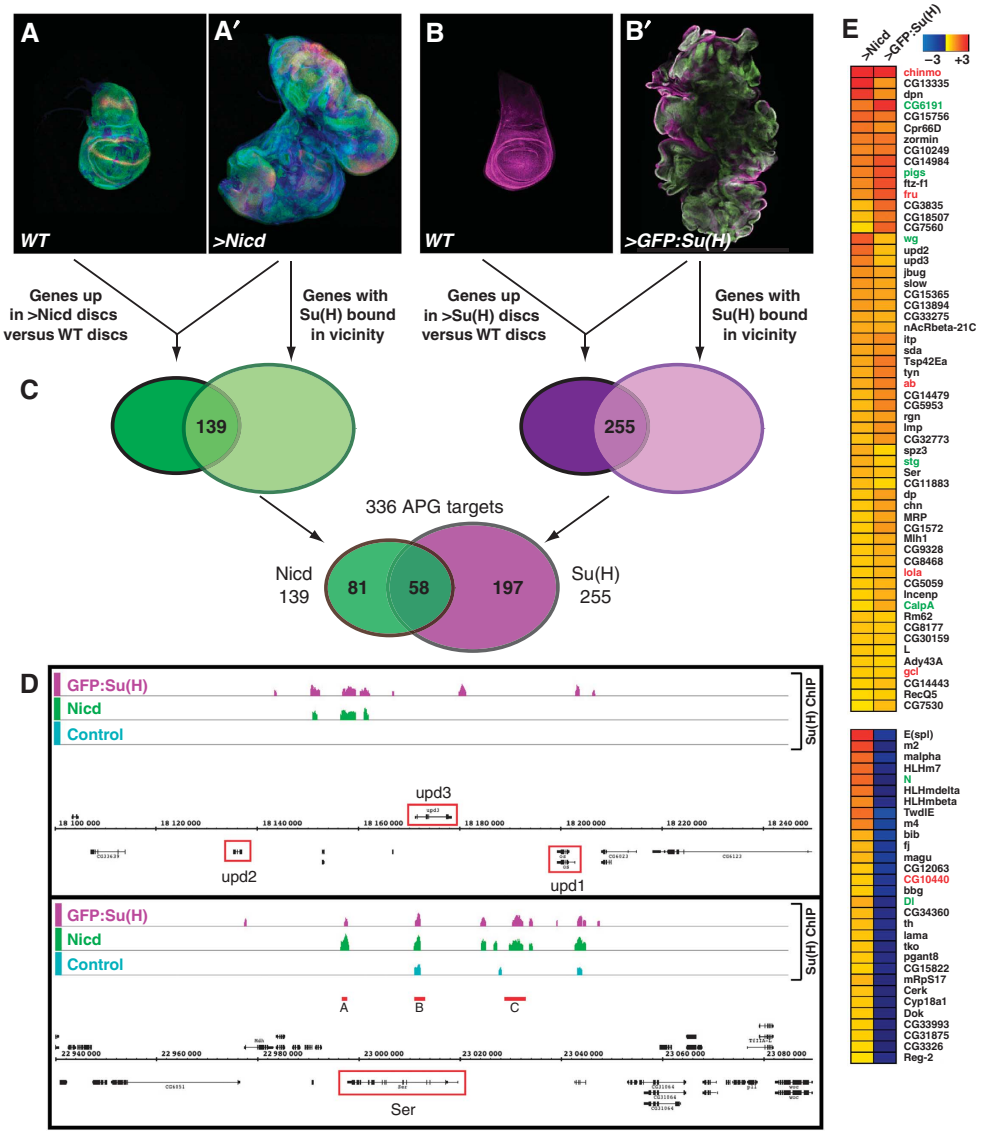

Figure 1 Identification of Notch regulated genes in proliferating epithelial wing imaginal discs cells. (**A**–**B**′) Wild-type wing discs and hyperplastic discs produced by manipulating Notch activity. (**A**, **A**′) Randomly generated clones of cells overexpressing GFP alone (**A**) or with Nicd (**A**′) in wing imaginal discs. Clones were marked with GFP (green), and tissue counterstained to detect E-Cadherin (blue) and Wg (red). (**B**, **B**′) *ptc-Gal4* control (**B**) or *ptc-Gal4* driven GFP:Su(H) fusion protein (green; **B**′); discs are counterstained with E-Cadherin (purple). (**C**) Strategy to identify direct Notch targets. Expression arrays were used to identify transcriptionally upregulated genes in the two genotypes (365 in Nicd; 460 in GFP:Su(H)) and ChIP was performed to locate Su(H) bound regions (2833 in Nicd; 4795 in GFP:Su(H)). Genes in the vicinity of ChIP peaks were identified, such that each peak may be associated to more than one gene and genes may be associated to more than one peak, generating a list of all neighbouring genes irrespective of orientation or distance cut-off (more details in Supplementary data). Venn diagrams illustrate the intersection of these two data sets, Assigned Peak Gene (APG) targets, for each genotype (that corresponded to 848 (30%) peaks from Nicd discs and 2232 (46%) peaks from GFP:Su(H)). Lower Venn diagram depicts the overlap between the APG targets from each. (**D**) Examples of genomic regions from two representative Notch APG targets showing Su(H) enriched regions (enrichment relative to input AvgM, scale log2 0–4) in wing discs from wild type (cyan), Nicd (green), and GFP:Su(H) (purple). Gene models are depicted in black, horizontal numbering indicates genomic coordinates, upregulated genes are boxed in red. Bottom panel: red lines (**A**: Ser_minimal_wing_enhancer; B: Ser_V-1.9; C: Ser_II-4.2) highlight identified enhancers for Notch regulated expression of *Serrate* at the D/V boundary (Bachmann and Knust, 1998; Yan *et al*, 2004). (**E**) Heat maps illustrating changes in expression of identified APG targets compared to wild type. (Top) Upregulation of common APG targets, ranked according to fold change in Nicd expressing discs; (Bottom) cluster of genes identified by hierarchical clustering that are upregulated in Nicd but downregulated in GFP:Su(H) discs. Genes in cell proliferation GO categories are highlighted in green and BTB/POZ genes are highlighted in red.

growth, and 3 to stem cell maintenance, in addition to those related to development and morphogenesis (e.g., wing disc development; Figure 2A).

Genes included in proliferation- and growth-related categories represented a broad spectrum. For example, proliferation-related genes ranged from those encoding secreted mitogens, such as *wg*, *Wnt6*, *upd2*, *upd3* (extracellular activators of Wnt/β-catenin and Jak/Stat pathways, respectively), to those encoding direct cell-cycle regulators, such as *Cyclin E* (*CycE*), *string/cdc25*, *Lk6*, and *polo*. Also included were *sd* and *vg*, which encode transcription factors with known roles in coordinating wing-disc growth (the former also acts as a transcription factor in the Hippo pathway) and novel candidates, such as *CG6191* and *Btk29A* (BTK Tec

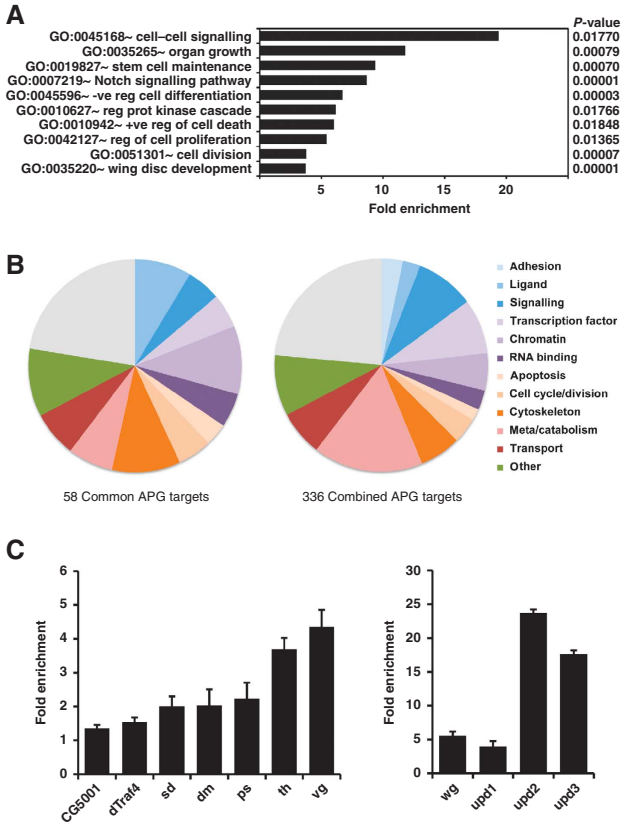

Figure 2 Characteristics and validation of Notch APG targets. (**A**) GO categories (Biological Process) enriched in the APG targets, ranked by *P*-values (calculated using a Hypergeometric test with Benjamini correction). Results were filtered for categories with ⩾3-fold enrichment and *P*-value⩽0.05, overlapping processes were grouped, and the most enriched depicted here. (**B**) Pie charts depicting proportions of genes with the indicated molecular functions for common APG targets (left) and for combined APG targets. Proportions are broadly similar except that adhesion and meta/catabolism constitute a larger component of the combined set, while ligand and cytoskeleton are commensurably reduced. (**C**) Fold change in expression levels between Nicd overexpressing discs and control discs for the indicated genes determined by qPCR. Expression levels were normalized to rp49 before calculating the fold change. Error bars indicate standard error of the mean (three biological replicates).

kinase homologue), whose homologues have been linked to proliferation (Anderson *et al*, 1996; Kirley *et al*, 2005). Similarly, the 'growth' genes encode core determinants of translation efficiency (*eIF-4a*) as well as secreted signals (*wg*, *hedgehog*). Thus, these combinations of targets potentially explain both autonomous and non-autonomous effects of Notch on proliferation and growth. As several, including *dm/myc*, were reportedly inhibited by Notch (Herranz *et al*, 2008) and/or unrelated to growth in wing discs, we selected a subset for validation (by quantitative RT–PCR). This independent analysis confirmed that their mRNA levels were upregulated in Nicd expressing discs (Figure 2C) and/or in Su(H) expressing discs (Supplementary Figure 1G).

Further stratification of gene functions revealed that the full spectrum of Notch responsive genes included regulators/components of cell adhesion, cytoskeleton, programmed cell death, and metabolism (Figure 2B). The latter were particularly prevalent in Su(H) hyperplastic discs. The target identities also demonstrated that Notch regulation of cell signalling occurs at many levels, as both positive and negative components of pathways were included. This is exemplified by one GO category, 'regulation of protein kinase cascade'. Most members belonged to the Jak/Stat pathway and they encoded repressors (*Socs36e* and *ken and barbie* (*ken*)) as well as positively acting ligands (*upd1*, *upd2*, and *upd3*).

Finally, an unexpected enrichment for BTB/POZ domain proteins was uncovered by the analysis of protein domains in APG (eight genes; five-fold enrichment, $P=0.00057$). Five such BTB/POZ genes (*ken*, *chinmo*, *abrupt* (*ab*), *lola*, and *fruitless*) also contain zinc-finger domains (POZ-ZF). Transcription factors of this class frequently function as repressors and have been linked to different developmental and tumorigenic processes (Kelly and Daniel, 2006). In flies, *lola* was shown to cooperate with *N* in regulating *E2f* (Ferres-Marco *et al*, 2006) and *chinmo* was found to contribute to tumorigenesis (Flaherty *et al*, 2010). A component of the Notch response may thus be achieved by regulating the chromatin landscape through these POZ-ZF proteins.

Notch targets are required for the induced overgrowth

To address whether identified Notch targets were relevant for the overgrowth, we used RNAi to mediate knock down of their expression in Nicd expressing cells (with *ptc-Gal4 Gal80ts*). As *ptc-Gal4* driven Nicd primarily causes elongation of the disc in one axis, we assessed the consequences by measuring the ratio between the A/P and D/V dimensions (Figure 3A and B; Nicd expressing discs have A/P > D/V with a ratio of 1.4; control discs have A/P < D/V with ratio of 0.7). We therefore anticipated that the knock-down of any genes important in mediating the overgrowth would shift the ratio in Nicd discs closer to that of control discs. Of the 20 genes tested in this way, the majority caused a reduction in the ratio indicative of their contribution to the overgrowth. The strongest effects were with knock-down of *sd* which fully suppressed the overgrowth to almost control levels, indicating an essential role downstream of Notch. Likewise, ablation of *string/cdc25*, *escargot*, and *wg* strongly suppressed the overgrowth (Figure 3C and E). Reduction in other targets had intermediate effects, for example, *Btk29A*, *fru*, *lola*, and *dm/myc* also significantly reduced the overgrowth while knock-down of any one of the *upd* genes caused a consistent mild reduction (Figure 3D and E).

Mutations affecting the Hairless (H) co-repressor ($H^2/+$) result in an increase in Notch signalling, producing adult wings that are larger than wild-type (Figure 3F and G). Changes in the levels of expression of novel targets might therefore modify the $H^2/+$ wing size phenotype. We therefore assessed whether we could detect any modifications in wing size by halving dosage of target genes using the smallest available mapped deficiencies. Such deletions had advantages of being definitive nulls and of allowing us to test the relevance of gene clusters, such as *outstretched-upd* (three related genes) and *wg-wnt* (containing four related genes), where recently duplicated genes have overlapping functions. Deficiencies for *Btk29A*, *dm*, *sd*, *upd1/2/3*, and *vfl* all suppressed the $H^2/+$ *phenotype*, further supporting the hypothesis that these genes act downstream of Notch (Figure 3H).

Subsequently, we examined the relevance to wing growth under normal conditions, ablating expression of targets in the posterior compartment (using *engrailed-Gal4*, *en-Gal4*) and

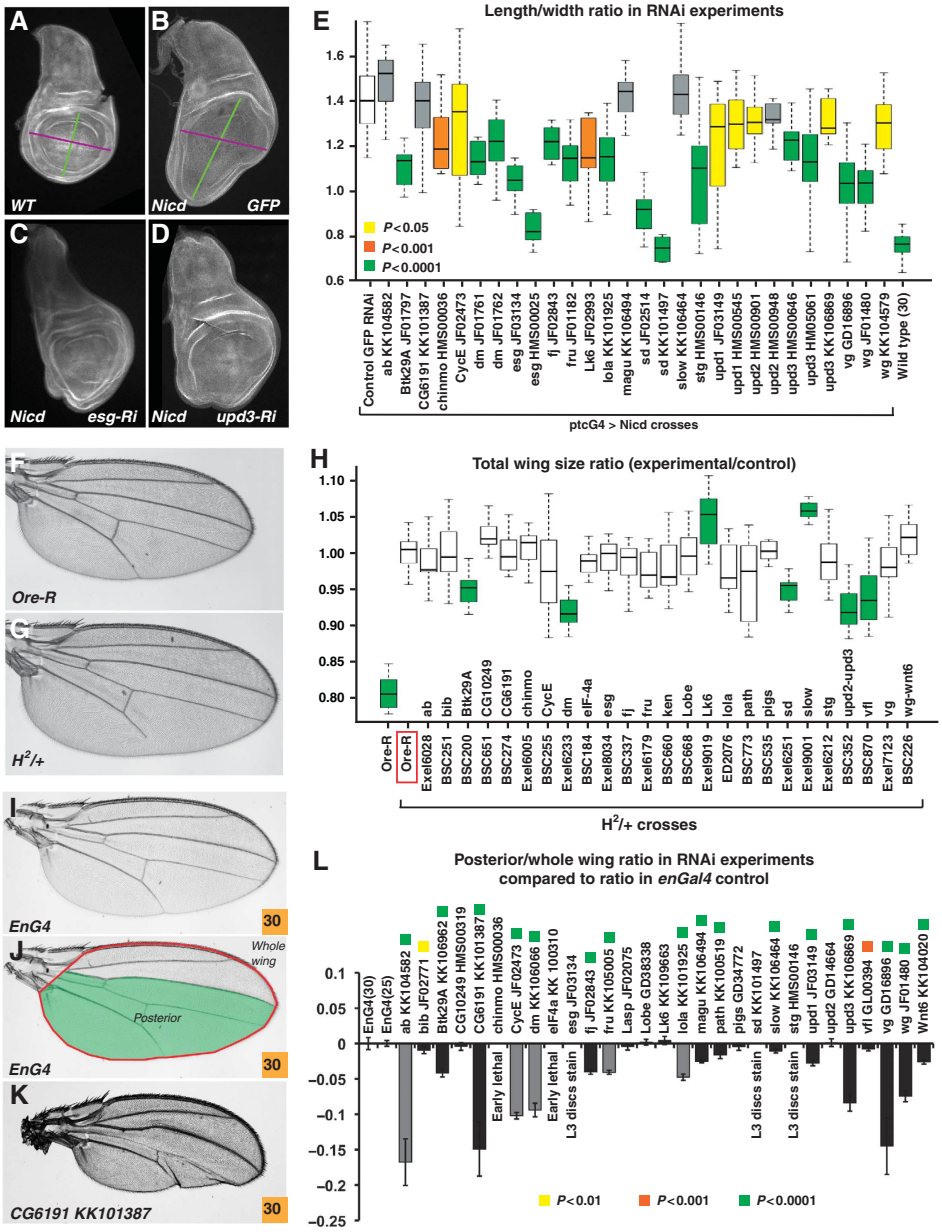

Figure 3 Functions of APG targets downstream of Notch and for wing size. (**A**–**D**) Third instar wing imaginal discs stained with E-Cadherin (white). (**A**) Wild-type *ptc-Gal4*, *tubGal80ts*/+ wing disc. (**B**) Wing discs from *ptc-Gal4, tubGal80ts* driving *UAS-Nicd* & *UAS-GFPRNAi* for 60 h at 30°C. (**A**, **B**) Green lines indicate the AP length and purple lines the DV width of the wing disc that were measured. The AP length/DV width ratio is 0.77 in wild type (**A**) and 1.41 in >Nicd (**B**). (**C**, **D**) Wing discs after Nicd overexpression together with RNAi mediated knock-down of *esg* (**C**; ratio = 1.05) or *upd3* (**D**; ratio = 1.14). (**E**) Effects of RNAi against the indicated genes on Nicd induced hyperplasia. Hyperplasia was quantified by calculating the ratio between the AP length (green line, **A**, **B**) and the orthogonal DV width (purple line, **A**, **B**). Ratios were calculated for 'wild-type' discs (*ptc-Gal4*, *tubGal80ts*), control discs (*ptc-Gal4*, *tubGal80ts* driving *UAS-Nicd* and *UAS-GFPRNAi*; labelled as control) and for discs expressing Nicd together with the different indicated RNAi. Box plot depicts the ratios obtained from wing discs of larvae grown at 30°C for 60 h. Significantly different results (unpaired two-tailed Student's *t*-test) are indicated according to the colours in the key. (**F**, **G**) Enlarged adult wings from *Hairless*^{2} heterozygote ($H^2/+$; **G**) compared to wings from *ORE-R* wild type (**F**). (**H**) Genetic interactions between APG and Notch pathway measured by effects of reducing gene dose on $H/+$ wing size. Box plot showing wing sizes from the indicated genotypes as a ratio to $H^2/+$ wings (red rectangle; note that *Ore-R* wild-type wings, left column, are circa 80% of $H^2/+$). Combinations that differed significantly ($P<0.05$, unpaired two-tailed *t*-test) from $H^2/+$ are shaded in green. (**I**–**K**) Adult wing phenotypes produced by targeting RNAi against Notch APG, as indicated, in the posterior of the wing using *en-Gal4*. (**I**, **J**) Wild-type *en-Gal4*/+ wing; (**J**) regions used to calculate growth effects in (**I**) are shown by green shading (posterior territory; L3 was used as the boundary to ensure consistent measurements) and red line (whole wing). (**K**) Phenotype produced by RNAi targeting *CG6191* at 30°C. (**L**) Effects of RNAi against the indicated genes on wing size. The ratio between the posterior territory (green, **J**) and the overall wing (red, **J**) was calculated for control wings (*en-Gal4*) and for RNAi expressing wings. Graph depicts the difference between RNAi and control ratios from flies grown either at 25°C (grey boxes) or at 30°C (black boxes). Significantly different results (Kolmogorov–Smirnov test) are indicated by coloured squares according to the key, error bars represent standard deviation. RNAi combinations that did not produce viable adults either survived to third instar larvae (L3 discs stain; see Supplementary Figure 3) or were lethal at earlier stages (early lethal).

assessing effects on wing size. By quantifying effects in the region affected by *en-Gal4* relative to total wing size, any differences arising from animal size variability were eliminated: the posterior to whole wing ratio of wild type (Figure 3I and J) was constant (0.706 ± 0.008) and independent of fly culture conditions. Of the 28 Notch regulated APG tested in this way (Figure 3L; Supplementary Figure 2; Supplementary Table 7), most resulted in reduced posterior wing size (17/23). Ablation of seven genes, including *vg*, *CG6191*, and *upd3*, led to strong reduction in size (Figure 3K; Supplementary Figure 2), four had a moderate effect (e.g., *Btk29a*, *four-jointed [fj]*, *lola*) and a further six showed a modest decrease (Figure 3L; Supplementary Figure 2; Supplementary Table 7). Several of the remainder caused lethality either at pupal stages (*sd*, *stg*, *esg*; with some producing detectable defects in the larval discs; Supplementary Figure 3) or earlier (*chinmo* and *eIF-4A*). Thus, many of the Notch APG are likely to contribute to tissue growth in normal development as well as in Notch induced hyperplasia.

Different spatial responses among Notch targets

Many of the downstream targets, such as *th*, *CycE*, *CG6191*, *Lk6*, and *chinmo*, have not hitherto been linked positively to Notch activity. We therefore investigated further the Notch regulation of these and several other novel targets, focusing on genes assigned to cell division, growth, or BTB/POZ clusters (15 loci in total). To accomplish this, we monitored expression from 'enhancer traps', P-element insertions in the different loci, comparing expression in wild-type and ectopic Nicd discs (using *ptc-Gal4*).

Interestingly, the responses could be stratified into four different patterns (Figure 4; Supplementary Figure 4). The first was a largely cell-autonomous response, where targets (*CG6191*, *ab*, and *wg*) were upregulated in a stripe in the centre of the pouch corresponding to the region where Nicd was being expressed (Figure 4C–E; Supplementary Figures 4A and 5A). This is the expected pattern for direct Notch targets. The second pattern was a stripe that extended more broadly through the wing pouch, arguing that it comprised both an autonomous and non-autonomous response (Figure 4F–H). The two genes in this group, *sd* and *fj*, are known to be Notch responsive genes. Our data indicate that they are direct targets and that their upregulation outside the Nicd expressing cells is likely to involve a secondary relay that could be mediated by Wg (Williams *et al*, 1993). The third group, including *th* and *CycE*, had a complex pattern with a narrow stripe of upregulation within the pouch and a broad upregulation at the peripheral tips (corresponding to hinge and pleural regions, Figure 4I–K; Supplementary Figures 4B–D and 5B). Their broad response in distal regions suggested that a signalling relay was also involved in their upregulation. They also appeared somewhat refractory to upregulation in the central wing pouch. Similar refractory component was exhibited by genes in group 4, such as *dm/myc* and *chinmo*, which were only upregulated in broad domains at the tips and not in the pouch (Figure 4L–N; Supplementary Figures 4E, F and 5C). Group 3 and group 4 genes thus appeared responsive to Nicd in a limited territory where their upregulation was detected in a diffuse domain suggestive of a relay mechanism.

To further confirm that targets were Notch responsive, expression of a subset (*wg*, *th*, *dm/myc*, *CycE*, and *chinmo*) was analysed in discs where Notch was ablated using RNAi. In all cases, expression was perturbed, although the regions affected differed according to the target (Supplementary Figure 6). For example, knock-down of Notch resulted in downregulation of *dm/myc* only at the periphery.

Su(H) binding identifies Notch responsive wing enhancers

The complex spatial responses led us to examine the function of the Su(H) occupied regions identified by ChIP. DNA fragments encompassing the Su(H) bound regions were therefore placed upstream of a minimal GFP reporter and the resulting expression patterns analysed in transgenic flies. First, DNA fragments from 'group 1' genes *cables/CG6191* and *wg* directed expression at the dorsal-ventral boundary, like the cognate gene, and recapitulated the response to Notch activation (Figure 5A–D). These results confirmed that the Su(H) bound regions identified Notch responsive enhancers (NREs), validating independently the ChIP results.

Second, fragments from 'group 3' genes *th/DIAP1*, *CycE* and *Lk6* were tested in a similar manner. The fragments from *th* and from *CycE* recapitulated fully the group 3 response of endogenous genes, with broad upregulation distally in Nicd expressing discs and a narrow stripe in the pouch (Figure 5F and H). These enhancers must therefore have the capacity to respond directly to Notch and to integrate additional inputs from the relay signal(s). To confirm that the complex response from the *CycE* enhancer included an element of direct Notch/Su(H) regulation, we mutated two conserved Su(H) sites within the fragment. The resulting reporter lacked expression at the normal D/V boundary (a site of endogenous Notch activity) and exhibited a compromised response to Nicd, with little upregulation at the distal tips and reduced expression in the A/P stripe (Figure 5I), suggesting that it receives direct regulation from Su(H) binding. Thus, even complex patterns of response, such as those exhibited by *th* and *CycE*, contain elements that depend directly on Notch/Su(H). The *Lk6* fragment differed from the others in that it failed to fully recapitulate the pattern from the enhancer trap in *Lk6*, instead being responsive throughout the Nicd stripe (Supplementary Figure 7; similar to group 1 gene fragments). One explanation for this difference is that other inputs, integrated elsewhere in the gene, modulate the expression of the Notch responsive *Lk6* enhancer to generate a 'group 3' response. However, further analysis would be needed to verify this hypothesis (including confirmation of endogenous *Lk6* mRNA expression).

Feed-forward signalling relays coordinate non-autonomous growth

Three of the four Notch response patterns (groups 2–4) implicate a secreted relay factor to account for the non-autonomous component of the response. Likely candidates among the Notch targets include *wg*, *Wnt6*, *upd2*, and *upd3*. High levels of Jak/Stat pathway activity, as measured by expression of a Stat92E-GFP reporter, were present at the peripheral regions in Nicd expressing discs (Supplementary Figure 4G; Bach *et al*, 2007). This corresponds to the domain where there was non-autonomous upregulation of group 3 and 4 targets, suggesting that *upd* genes (encoding the Jak/Stat pathway ligands) could be responsible for this relay mechanism. To investigate this possibility, we first

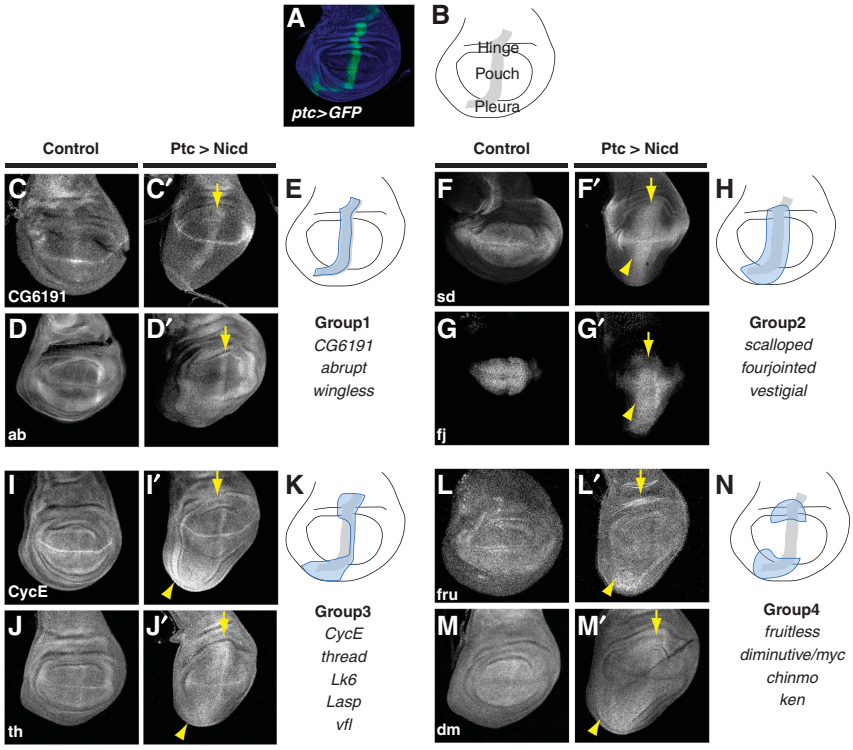

Figure 4 Notch APG targets exhibit different patterns of response. (**A**, **B**) Expression domain of *ptc-Gal4* visualized by driving GFP (green in **A**; E-Cadherin staining in blue), and schematized in (**B**) (grey); the stripe of expressing cells along the A/P boundary extends from the central wing pouch into the peripheral hinge and pleura. (**C**–**N**) Differing responses of Notch APG target genes to Nicd could be grouped into four classes, as indicated by the schematics (**E**, **H**, **K**, **N**) where blue shading approximates the response pattern in relation to the *ptc-Gal4* domain (grey). Expression was monitored via *LacZ* enhancer traps (**C**, **G**, **I**, **J**, **L**, **M**), *GFP* enhancer trap (**F**), or by antibody staining (**D**) in control wild-type wing discs (**C**–**M**) and in Nicd expressing discs (using *ptc-Gal4*; yellow arrows, **C**′–**M**′). (**C**–**E**) Group 1 response, illustrated by *CG6191* (**A**) and *ab* (**B**), consisted of upregulation within *ptc-Gal4* domain (yellow arrows **C**′, **D**′, blue territory **E**). Other genes with this response profile are listed with the schematic in (**E**). (**F**–**H**) Group 2 response, illustrated by *sd* (**F**) and *fj* (**G**), consisted of upregulation within the *ptc-Gal4* domain (yellow arrows **F**′, **G**′), and in adjacent regions (yellow arrowheads **F**′, **G**′). Schematized in (**H**). (**I**–**K**) Group 3 response, illustrated by *CycE* (**I**) and *th/DIAP1* (**J**), consisted of upregulation primarily within peripheral portion of *ptc-Gal4* domain (yellow arrows **I**′, **J**′) and adjacent territories (yellow arrowheads **I**′, **J**′), but with narrow pouch stripe. Other genes with this response profile are listed with the schematic in (**K**). (**L**–**N**) Group 4 response, illustrated by *fruitless* (**L**) and *dm/myc* (**M**), consisted of upregulation only within peripheral portion of *ptc-Gal4* domain (yellow arrows **L**′, **M**′) and adjacent territories (yellow arrowheads **L**′, **M**′). Other genes with this response profile are listed with the schematic in (**N**).

analysed the consequences of Upd expression, using *ptc-Gal4 tub-Gal80ts*. The resulting wing discs were overgrown and there was widespread upregulation of both *dm/myc* (group 3) and *DIAP1/th* (group 4) as monitored by the *LacZ* enhancer trap lines (Figure 6A–E). This upregulation occurred broadly throughout the disc, beyond the stripe of Upd expression. Second, we asked whether any of the genes were associated with binding sites for Stat92E, the transcription factor in the pathway. Many Stat92E targets contain paired binding sites, to accommodate a dimer of Stat92E (Flaherty *et al*, 2009). Three out of four group 4 genes and one of the six group 3 genes (*DIAP1/th*; Figure 6M; Betz *et al*, 2008) were associated with paired Stat92E sites reinforcing the suggestion that Upd ligands could be one of the relay signals. The fact that not all group 3 and 4 genes have paired Stat92E sites may be explained if there are different Stat binding motifs and/or additional relay signals.

Feed-forward regulation by Sd and E(spl) refines the pattern of growth

A second feature of the Notch response in group 3 and 4 genes was a refractory region in the central wing pouch (Figure 4K and N). As genes in groups 1 and 2 exhibited a complementary response, responding primarily within the pouch territory (Figure 4E and H), we hypothesized that one or more of the genes in groups 1 or 2 could be responsible for preventing upregulation of group 3 and 4 genes in the wing pouch. One candidate was *sd*, a key downstream effector as illustrated by its ability to suppress the Nicd phenotype (Figure 3E).

Sd is a group 2 Notch target that encodes a transcription factor implicated in growth control through the formation of transcriptional complexes with Vg (Halder *et al*, 1998; Simmonds *et al*, 1998), or Yki, the transcriptional activator of the Hippo pathway (Goulev *et al*, 2008; Wu *et al*, 2008). Strikingly, when we combined RNAi mediated knock-down of *sd* or *vg* together with the overexpression of Nicd (using *ptc-Gal4 Gal80ts*), we observed an upregulation of *th* and *dm* in the central wing pouch (Figure 6H–L), arguing that the increased Sd and Vg levels after Notch activation prevent their response in the central wing pouch in agreement with our hypothesis.

Similarly, *E*(*spl*) bHLH genes are well-characterized Notch targets that encode powerful bHLH transcriptional repressors and respond with characteristics of group 1 genes (Cooper *et al*, 2000). When overexpressed with *ptc-Gal4*, E(spl)m8 inhibited the expression of *dm/myc* (group 4; Figure 6C).

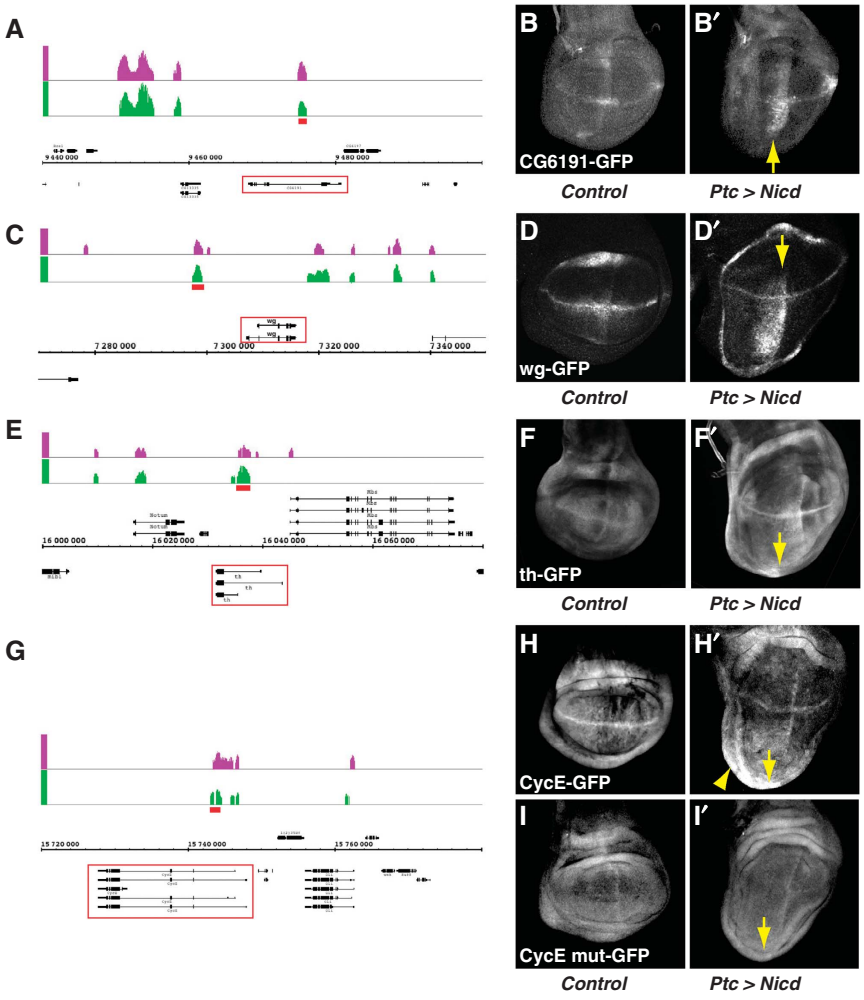

Figure 5 Su(H) bound regions identify Notch responsive enhancers in APG targets. (**A**, **C**, **E**, **G**) Genomic regions from indicated Notch APG targets showing Su(H) enriched regions (enrichment relative to input, AvgM, scale log2 0–4) in wing discs from Nicd (green) or GFP:Su(H) (purple). Gene models are depicted in black, horizontal numbering indicates genomic coordinates, the upregulated genes are boxed in red, and the DNA fragments tested for their Notch pathway sensitivity in (**B**, **D**, **F**, **H**, **I**) are indicated by red rectangle above. (**B**, **D**, **F**, **H**) Patterns of GFP expression generated by enhancers from the indicated genes in control (**B**, **D**, **F**, **H**) and Nicd expressing (**B′**, **D′**, **F′**, **H′**) discs. Fragments depicted in (**A**, **C**, **E**, **G**) were inserted upstream of minimal promoter fused to GFP and the resulting expression patterns examined in transgenic flies in the absence or presence of ectopic Nicd as indicated. Arrows indicate the stripe of Nicd expression (*ptc-Gal4* stripe). All four enhancers are upregulated, recapitulating some or all of the expression from cognate gene (see Figure 4). (**I**) Mutation of Su(H) binding motifs in *CycE* enhancer compromises expression. Two conserved Su(H) binding motifs were identified. Site-directed mutagenesis resulted in an enhancer giving no basal expression at the DV boundary (**I**) and little residual response to ectopic Nicd (**I′**, yellow arrows).

Feed-forward regulation by E(spl) repressors could therefore explain why *dm-LacZ* was only upregulated by Nicd at the periphery. Expression of *DIAP1/th* (group 3) was however not downregulated by E(spl)m8 expression (Figure 6F), showing that different Notch targets have different feed-forward inputs.

Taken together, these results suggest that transcription factors such as E(spl)m8, Vg, and Sd, which are targets of Notch, feed forward onto other Notch targets such as *th* and *dm* to pattern their responses, thus creating a refractory zone for group 3 and 4 genes in the central wing pouch.

Discussion

By considering the overlap of two independent genomic approaches, transcriptome profiling and whole genome Su(H) occupancy, we have identified a set of 336 direct Notch target genes that potentially contribute to hyperplasia caused by elevated Notch activity in *Drosophila* wing discs. Indeed in functional tests, the majority of those tested could suppress the overgrowth. In addition to well-established growth regulators such as *dm/myc*, *string/cdc25*, and *CyclinE*, novel genes such as *Btk29A* and *CG6191* (the *Drosophila* homologue of *CABLES1/2* (Cdk5 and ABL substrate)) were also upregulated. Notably, several of the targets are homologous to genes that have been identified in studies of Notch regulated genes in human cancer cells (Mazzone *et al*, 2010; Wang *et al*, 2011). First, *MYC* (*dm*) and *CDC25* (*stg*) are conserved targets in the majority of contexts analysed, including T-ALL and mammary cells (Klinakis *et al*, 2006; Palomero *et al*, 2006; Sharma *et al*, 2006; Weng *et al*, 2006; Mazzone *et al*, 2010). Second, a significant number of genes upregulated by an activated form of NOTCH1 in mammary epithelium-derived MCF-10A cells (Mazzone *et al*, 2010) have homologues among our APG targets (56/795 upregulated human genes, $P<0.0017$;

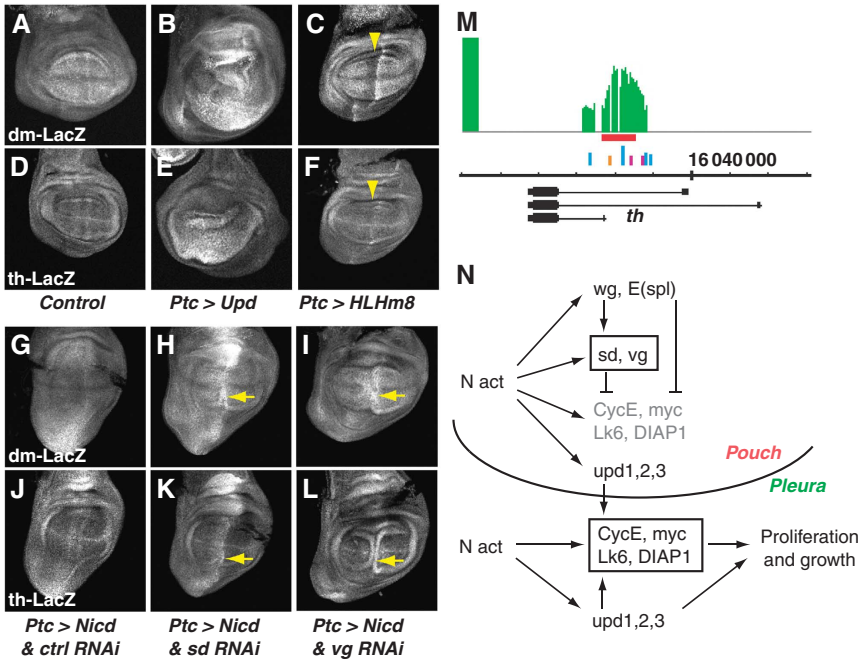

Figure 6 Cross-regulatory interactions between targets shape the response patterns. (**A–L**) Effects of *upd*, *E*(*spl*)*m8*, *sd RNAi*, and *vg RNAi*, on expression of *myc-lacZ* (*dm-lacZ*; **A–C**, **G–I**) and *DIAP1/th-lacZ* (*th-lacZ*; **D–F**, **J–L**) in the indicated conditions compared to wild type (**A**, **D**). Expression of Upd promotes expression of *dm-lacZ* (**B**) and *th-lacZ* (**E**) whereas expression of E(spl)m8 inhibits *dm-lacZ* but not *th-lacZ* (**C**, **F**, yellow arrowheads). Upregulation of *dm-lacZ* and *th-lacZ* by Nicd is restricted to the periphery (**G**, **J**) but when *sd* (*sd* RNAi; **H**, **K**) *or vg* (vg RNAi; **I**, **L**) is simultaneously ablated both *dm-lacZ* and *th-lacZ* activation occurs more broadly in the pouch (**H**, **K**, **I**, **L** yellow arrows). (**M**) Motifs located within the *th/DIAP1* NRE indicate the potential for regulatory input in the wing discs. Genomic region from *th/DIAP1* showing Su(H) bound region in Nicd overexpressing disc (green) in relation to conserved Su(H) binding motifs (blue), validated solo Sd binding site responsive to the Hippo pathway (orange; Wu *et al*, 2008), and validated tandem Stat92E sites responsive to the Jak/Stat pathway (purple; Betz *et al*, 2008). Gene models are depicted in black and horizontal numbering indicates genomic coordinates. (**N**) Model of regulatory network downstream of ectopic Notch activation (*N act*) that shapes the proliferative response. Upregulation of diffusible signals (*wg* and *upd*) and feed-forward repression (e.g., *sd* and *vg*) are proposed to act in combination with Notch at many targets (e.g., *dm/myc* and *th/DIAP1*) so that overgrowth occurs predominantly at the periphery (hinge and pleura). This is a simplified model, and we note that some targets (*th* and *cycE*) are also expressed at sites of endogenous N activity in the wing pouch (d/v boundary).

Supplementary Table 8). These include ligands of the *IL6* (*upd*) and *WNT* (*wg*) families as well as *TEAD* (*sd*), and *VGLL* (*vg*) transcriptional regulators. Thus, aspects of the network described in *Drosophila* wing discs could be relevant for Notch-driven mammary cell proliferation.

Previous studies have indicated that Notch regulates growth autonomously, within the cells where it is activated, and non-autonomously, in the surrounding cells. GO analysis revealed how the Notch targets could explain these direct and indirect effects. First, several proliferation and growth-related categories were significantly enriched. Second, the constituent genes were not only involved directly in cell-cycle progression/growth (*stg*, *CycE*, *myc*), but also in producing secreted ligands (e.g., Wnts and Upds). These genes thus provide a molecular mechanism for the observed effects of Notch in regulating tissue growth. In addition, there was significant enrichment of unexpected categories, most notably genes encoding BTB/POZ domain proteins such as *chinmo* and *lola*. The former has been linked to hyperplasia in other *Drosophila* tissues in part downstream of the Jak/Stat pathway (Flaherty *et al*, 2010) although the mechanisms are not yet known.

Analysis of target gene regulation further emphasized the autocrine and paracrine effects of Notch. Thus in only a few cases was the upregulation of tested targets restricted to the cells expressing activated Notch. Such targets included *wg*, which is known to act downstream of Notch (Diaz-Benjumea and Cohen, 1995; Rulifson and Blair, 1995; de Celis *et al*, 1996), and *CG6191*. We note that, although widely considered as a Notch direct target, this is the first demonstration of Su(H) binding and the first identification of NREs in the *wg* locus. However, the majority of targets tested were also upregulated in some neighbouring cells. This non-autonomy showed two patterns. In one, it flanked the misexpressing cells along much of the Nicd expression domain. In the other, it occurred primarily at the periphery. The former may be attributed to Wg as genes exhibiting this pattern include *sd* and *vg*, previously suggested to have input from Wg signalling (Williams *et al*, 1993; Neumann and Cohen, 1996). The latter is most likely due to Upd ligands because the peripheral regions exhibit expression of a Jak/Stat pathway sensor. In agreement, paired STAT motifs were detected in several target genes that showed peripheral upregulation and ectopic Upd expression was sufficient to upregulate two genes tested. Similar synergies may also be relevant in Notch fuelled solid tumours because Notch activation in MCF10A breast cancer cells (*via* overexpression of NICD1), led to overgrowths that were sensitive to Jak/Stat signalling. Homologues of the Upd ligands (*IL6*) were among the genes overexpressed under these conditions (Mazzone *et al*, 2010).

A further feature of many of the hyperplasia-related Notch targets, such as *dm/myc*, *CycE*, and *DIAP1/th*, was that they were only upregulated by Nicd at the periphery and not in the

central regions. This implies the existence of a repressive mechanism that counters the inductive Notch signal. Strikingly, knock-down of the centrally upregulated Notch targets *sd* or *vg* was able to restore expression of *dm/myc* and *th/DIAP1* throughout the Nicd expressing territory, suggesting that Sd and Vg are part of a feed-forward repression mechanism that inhibits upregulation of other targets in the central domain. Sd is a TEA domain DNA binding protein that regulates transcription through interactions with different co-factors, Vg (Halder *et al*, 1998; Simmonds *et al*, 1998) and Yki (Goulev *et al*, 2008; Wu *et al*, 2008). The exact outcome on transcription depends on the relative amounts of these three transcription factors. For instance, interactions with Vg appear to switch the Sd binding-site preference to favour tandem sites, possibly at the expense of targets with solo Sd motifs (Halder and Carroll, 2001; Garg and Bell, 2010). The functional Sd site in *th* is a solo site responsive to the Hippo pathway (Wu *et al*, 2008). Thus by altering levels of Sd and Vg, Notch activation could bias against expression of genes with solo Sd sites in the central territory. *Myc/dm* is also repressed in the central region and is a target of Sd-Yki, although it is not clear whether through a solo site (Neto-Silva *et al*, 2010). TEAD2, the vertebrate homologue of Sd, was recently identified as a transcriptional target of the Notch pathway in mouse neural stem cells, suggesting that a similar interaction between Notch and the Hippo pathways could occur in vertebrates (Li *et al*, 2012). The proposed regulatory network also extends an earlier model that Sd is essential in coordinating the expression of multiple targets in wing development (so-called Selector gene; Guss *et al*, 2001) by incorporating the feed-forward regulation by Notch as well as the relevance of Sd levels and inhibitory aspects of Sd function that have been suggested by other studies (e.g., Halder *et al*, 1998).

In identifying the Notch regulated genes we have taken a parsimonious approach, using the intersection between genes with significantly upregulated transcripts and genes in the proximity of Su(H) bound regions. Strikingly, the peaks of Su(H) occupancy were frequently clustered and many of these overlapped between Nicd expressing and Su(H) expressing discs. It is also notable that many Su(H) bound regions were not associated with genes whose expression was detectably altered under either regime. Some of this may be attributed to genes where the expression was variable between discs, or was restricted to limited domains, so that the changes were not sufficiently reproducible. Of more interest is the possibility that the associated genes were not responsive under the conditions used due to the presence of repressors (Wang *et al*, 2011) or absence of co-activators. Finally, we identified a small cohort of genes that were upregulated by Nicd but downregulated by Su(H) overexpression. This difference could arise due to the different experimental paradigms but it may also be indicative that the tertiary complex of Su(H) with Nicd and Mastermind is essential for the upregulation of these particular genes (such that Su(H) overexpression titrates away this activator complex; Furriols and Bray, 2000). In contrast, outcompetition of co-repressor complexes may be sufficient to cause the upregulation of genes that are highly upregulated in the Su(H) discs which include many of the growth regulatory targets. If so, then Notch may be permissive for their expression, rather than instructive, potentially explaining the observation that the regulation of these targets is highly sensitive to synergies with other factors, such as Jak/Stat signalling, and is susceptible to inhibition from Sd or E(spl)m8.

Materials and methods

Drosophila genetics

Overproliferating third instar larval wing discs were generated (i) by overexpressing *UAS-Nicd* in randomly generated clones in progeny from *abxUbxFLPase*; *Act>y>Gal4, UAS GFP*; *FRT82B tubGal80 x UAS-Nicd*; *FRT82B* (which gives a high frequency of Nicd expressing clones throughout the wing disc ensuring penetrant phenotypes for the genome-wide analysis and avoids bias that might be caused by driving expression only in one area) (ii) by overexpressing *UAS-GFP:Su*(*H*) with the *patched[559.1]-Gal4* driver (*ptc-Gal4*).

Response of Notch APG targets was analysed by crossing *ptc-Gal4, tubGal80ts*; *UAS-Nicd* (or *UAS-Su*(*H*), or *UAS-N RNAi*) with *lacZ* or *GFP* enhancer trap lines (see Supplementary data). Crosses were cultured at 20°C for 7 days, then shifted to 30°C (non-permissive temperature for Gal80ts) for 60 h before dissection and staining. Similar regime was used in combination with UAS-RNAi lines (from Bloomington or VDRC stock centers) for quantifying effects of target gene knock down before dissection, mounting, and measuring of the width and length of the wing discs as indicated in Figure 3, 10–30 imaginal discs were scored for each genotype.

Function of the Notch target genes during normal wing growth was analysed by crossing the indicated RNAi lines with *engrailed[e16E]-Gal4* driver (*en-Gal4*). Crosses were cultured for 3 days at 25°C, then shifted to 30°C or left at 25°C (if lethality was observed at 30°C); adult wings were then mounted and measured.

Expression arrays and ChIP

Expression analysis and ChIP experiments were performed and analysed as described previously (Krejcí *et al*, 2009) with the following modifications: (i) For each biological replicate RNA obtained from 60 wing discs was reverse transcribed and hybridized on long-oligonucleotide FL003 INDAC micro-arrays representing 14 444 transcripts from release 5 of the *Drosophila* genome. (ii) For each biological replicate, Su(H) ChIP products were obtained from 180 wing discs amplified and hybridized to NimbleGen *D. melanogaster* 2.1 M Whole-Genome Tiling Arrays. Details of normalization and peak identification are in Supplementary data. Results have been deposited in Gene Expression Omnibus with series accession number GSE41429 (GEO, http://www.ncbi.nlm.nih.gov/geo/).

Quantitative RT–PCR

RNA from 60 dissected third instar larva wing discs of control and overproliferating discs was extracted using TriZOL. Genomic DNA was eliminated using Ambion's DNA-free kit (#AM1906). cDNA was synthesized using random hexamers (Promega #C118A) and M-MLV reverse transcriptase (Promega #M170B). Quantitative PCR was then performed using QuantiTect SYBR Green PCR Kit (QIAGEN #204145) with a Roche Light Cycler. Samples were normalized using the Rp49 gene as control. Primers are detailed in Supplementary data.

Reporter assays

Putative NREs in *CG6191*, *CycE*, and *Lk6* were cloned in the *pGreenRabbit* vector (*pGR*) (Housden *et al*, 2012). Release 5 coordinates of the cloned fragments were *CG6191*, chr2R: 9 474 750–9 475 941; *wg*, chr2L:7 295 440–7 301 567; *th*, chr3L:16 035 761 –16 036 948; *Lk6*, chr3R:7 586 176–7 587 411; *CycE*, chr2L: 15 743 005–5 744 522. The mutated Su(H) motifs in *CycE* were at positions 15 743 162 (TTCCCACA mutated to TaaCaACA) and 15 743 998 (CGTGTGAA mutated to CGTtGttA). Flies carrying the *pGR* transgenes were generated by Phi-C31 mediated site-directed integration on the 86Fb platform. The Notch pathway responsiveness of cloned enhancers was analysed as above.

Immunofluorescence

Immunostainings were performed according to standard protocols. Antibodies used were mouse anti-Ab (Developmental Studies Hybridoma Bank—DSHB Ab; 1/25), rat anti-Ci (DSHB 2A1; 1/25),

mouse anti-Cut (DSHB 2B10; 1/25), mouse anti-Dlg (DSHB 4F3; 1/25), rat anti-ECad (DSHB DCAD2; 1/25), mouse anti-β-Galactosidase (DSHB 40-1a; 1/25), mouse anti-Wg (DSHB 4D4; 1/25), rabbit anti-CycE (Santa Cruz sc-33748; 1/500), guinea-pig anti-Dpn (gift from Jim Skeath; 1/2000), guinea-pig anti-dm (gift from Gines Morata; 1/500), rabbit anti-cleaved Caspase 3 (D175) (Cell Signaling Technology 9661; 1/500), rabbit anti-GFP (Molecular Probes A6455; 1/2000), and rabbit anti-phospho-Histone3 (Ser10) (Upstate 06-570; 1/500).

Wing measurements

In all, 15–20 wings from independent females were mounted, imaged, and measured using ImageJ. For quantification of RNAi effects, the posterior region (p) and total wing (w) size were measured. The ratio p/w was then compared between experimental RNAi and *en-Gal4* controls, and the statistical significance determined using non-parametric Kolmogorov–Smirnov test. For *H* genetic interactions, four virgin females of $H^2/TM6B$ were crossed to four males of the indicated deficiencies (reversed for X chromosome deficiencies). After 4 days, G0 flies were removed to avoid overcrowding from excess progeny. Unpaired, two-tailed Student's *t*-test was used on raw wing measurements to assess whether differences were significant.

Supplementary data

Supplementary data are available at *The EMBO Journal* Online (http://www.embojournal.org).

Acknowledgements

We thank Bettina Fischer (FlyChip) and Audrey Fu for help with data processing; Agnes Le Foll for contributions to the RNAi experiments; other members of the Bray laboratory for valuable discussions; Gines Morata and Jim Skeath for antibodies. We acknowledge the Bloomington Stock Center, the DGRC Kyoto Stock Center, the VDRC Stock Center, and the Developmental Studies Hybridoma Bank for flies and antibodies. This work was supported by an MRC Programme grant to SJB (G0800034/1) and by a project grant from the Wellcome Trust to SJB and AD (WT083576MA). SF was supported by funding from BBSRC, Cambridge Overseas Trust, Zdenek Bakala Foundation, and Sackler Foundation.

Conflict of interest

The authors declare that they have no conflict of interest.

References

Anderson JS, Teutsch M, Dong Z, Wortis HH (1996) An essential role for Bruton's [corrected] tyrosine kinase in the regulation of B-cell apoptosis. *Proc Natl Acad Sci USA* **93:** 10966–10971

Bach EA, Ekas LA, Ayala-Camargo A, Flaherty MS, Lee H, Perrimon N, Baeg G-H (2007) GFP reporters detect the activation of the Drosophila JAK/STAT pathway *in vivo*. *Gene Expr Patterns* **7:** 323–331

Bachmann A, Knust E (1998) Dissection of cis-regulatory elements of the Drosophila gene Serrate. *Dev Genes Evol* **208:** 346–351

Baonza A, Garcia-Bellido A (2000) Notch signaling directly controls cell proliferation in the Drosophila wing disc. *Proc Natl Acad Sci USA* **97:** 2609–2614

Betz A, Ryoo HD, Steller H, Darnell Jr JE (2008) STAT92E is a positive regulator of Drosophila inhibitor of apoptosis 1 (DIAP/1) and protects against radiation-induced apoptosis. *Proc Natl Acad Sci USA* **105:** 13805–13810

Bray SJ (2006) Notch signalling: a simple pathway becomes complex. *Nat Rev Mol Cell Biol* **7:** 678–689

Cooper MT, Tyler DM, Furriols M, Chalkiadaki A, Delidakis C, Bray S (2000) Spatially restricted factors cooperate with Notch in the regulation of Enhancer of split genes. *Dev Biol* **221:** 390–403

de Celis JF, Garcia-Bellido A, Bray SJ (1996) Activation and function of Notch at the dorsal-ventral boundary of the wing imaginal disc. *Development* **122:** 359–369

Diaz-Benjumea FJ, Cohen SM (1995) Serrate signals through Notch to establish a Wingless-dependent organizer at the dorsal/ventral compartment boundary of the Drosophila wing. *Development* **121:** 4215–4225

Ferres-Marco D, Gutierrez-Garcia I, Vallejo DM, Bolivar J, Gutierrez-Aviño FJ, Dominguez M (2006) Epigenetic silencers and Notch collaborate to promote malignant tumours by Rb silencing. *Nature* **439:** 430–436

Flaherty MS, Salis P, Evans CJ, Ekas LA, Marouf A, Zavadil J, Banerjee U, Bach EA (2010) chinmo is a functional effector of the JAK/STAT pathway that regulates eye development, tumor formation, and stem cell self-renewal in Drosophila. *Dev Cell* **18:** 556–568

Flaherty MS, Zavadil J, Ekas LA, Bach EA (2009) Genome-wide expression profiling in the Drosophila eye reveals unexpected repression of Notch signaling by the JAK/STAT pathway. *Dev Dyn* **238:** 2235–2253

Furriols M, Bray S (2000) Dissecting the mechanisms of Suppressor of Hairless function. *Dev Biol* **227:** 520–532

Garg A, Bell J (2010) Reexamining the DNA target selectivity of Scalloped. *Genome* **53:** 575–584

Giraldez AJ, Cohen SM (2003) Wingless and Notch signaling provide cell survival cues and control cell proliferation during wing development. *Development* **130:** 6533–6543

Go MJ, Eastman DS, Artavanis-Tsakonas S (1998) Cell proliferation control by Notch signaling in Drosophila development. *Development* **125:** 2031–2040

Goulev Y, Fauny JD, Gonzalez-Marti B, Flagiello D, Silber J, Zider A (2008) SCALLOPED interacts with YORKIE, the nuclear effector of the hippo tumor-suppressor pathway in Drosophila. *Curr Biol* **18:** 435–441

Guss KA, Nelson CE, Hudson A, Kraus ME, Carroll SB (2001) Control of a genetic regulatory network by a selector gene. *Science* **292:** 1164–1167

Halder G, Carroll SB (2001) Binding of the Vestigial co-factor switches the DNA-target selectivity of the Scalloped selector protein. *Development* **128:** 3295–3305

Halder G, Polaczyk P, Kraus ME, Hudson A, Kim J, Laughon A, Carroll S (1998) The Vestigial and Scalloped proteins act together to directly regulate wing-specific gene expression in Drosophila. *Genes Dev* **12:** 3900–3909

Herranz H, Pérez L, Martín FA, Milán M (2008) A Wingless and Notch double-repression mechanism regulates G1-S transition in the Drosophila wing. *EMBO J* **27:** 1633–1645

Housden BE, Millen K, Bray SJ (2012) Drosophila reporter vectors compatible with ΦC31 integrase transgenesis techniques and their use to generate new Notch reporter fly lines. *G3* **2:** 79–82

Joshi I, Minter LM, Telfer J, Demarest RM, Capobianco AJ, Aster JC, Sicinski P, Fauq A, Golde TE, Osborne BA (2009) Notch signaling mediates G1/S cell-cycle progression in T cells via cyclin D3 and its dependent kinases. *Blood* **113:** 1689–1698

Kelly KF, Daniel JM (2006) POZ for effect—POZ-ZF transcription factors in cancer and development. *Trends Cell Biol* **16:** 578–587

Kim J, Sebring A, Esch JJ, Kraus ME, Vorwerk K, Magee J, Carroll SB (1996) Integration of positional signals and regulation of wing formation and identity by Drosophila vestigial gene. *Nature* **382:** 133–138

Kirley SD, Rueda BR, Chung DC, Zukerberg LR (2005) Increased growth rate, delayed senescence and decreased serum dependence characterize cables-deficient cells. *Cancer Biol Ther* **4:** 654–658

Klinakis A, Szabolcs M, Politi K, Kiaris H, Artavanis-Tsakonas S, Efstratiadis A (2006) Myc is a Notch1 transcriptional target and a requisite for Notch1-induced mammary tumorigenesis in mice. *Proc Natl Acad Sci USA* **103:** 9262–9267

Kopan R, Ilagan MXG (2009) The canonical Notch signaling pathway: unfolding the activation mechanism. *Cell* **137:** 216–233

Krejcí A, Bernard F, Housden BE, Collins S, Bray SJ (2009) Direct response to Notch activation: signaling crosstalk and incoherent logic. *Sci Signal* **2:** ra1

Krejcí A, Bray S (2007) Notch activation stimulates transient and selective binding of Su(H)/CSL to target enhancers. *Genes Dev* **21:** 1322–1327

Li Y, Hibbs MA, Gard AL, Shylo NA, Yun K (2012) Genome-wide analysis of N1ICD/RBPJ targets *in vivo* reveals direct transcriptional regulation of Wnt, SHH, and hippo pathway effectors by Notch1. *Stem Cells* **30:** 741–752

Ling H, Sylvestre J-R, Jolicoeur P (2010) Notch1-induced mammary tumor development is cyclin D1-dependent and correlates with expansion of pre-malignant multipotent duct-limited progenitors. *Oncogene* **29:** 4543–4554

Liu J, Sato C, Cerletti M, Wagers A (2010) Notch signaling in the regulation of stem cell self-renewal and differentiation. *Curr Top Dev Biol* **92:** 367–409

Mazzone M, Selfors LM, Albeck J, Overholtzer M, Sale S, Carroll DL, Pandya D, Lu Y, Mills GB, Aster JC, Artavanis-Tsakonas S, Brugge JS (2010) Dose-dependent induction of distinct phenotypic responses to Notch pathway activation in mammary epithelial cells. *Proc Natl Acad Sci USA* **107:** 5012–5017

Neto-Silva RM, de Beco S, Johnston LA (2010) Evidence for a growth-stabilizing regulatory feedback mechanism between Myc and Yorkie, the Drosophila homolog of Yap. *Dev Cell* **19:** 507–520

Neumann CJ, Cohen SM (1996) A hierarchy of cross-regulation involving Notch, wingless, vestigial and cut organizes the dorsal/ventral axis of the Drosophila wing. *Development* **122:** 3477–3485

Palomero T, Lim WK, Odom DT, Sulis ML, Real PJ, Margolin A, Barnes KC, O'Neil J, Neuberg D, Weng AP, Aster JC, Sigaux F, Soulier J, Look AT, Young RA, Califano A, Ferrando AA (2006) NOTCH1 directly regulates c-MYC and activates a feed-forward-loop transcriptional network promoting leukemic cell growth. *Proc Natl Acad Sci USA* **103:** 18261–18266

Ranganathan P, Weaver KL, Capobianco AJ (2011) Notch signalling in solid tumours: a little bit of everything but not all the time. *Nat Rev Cancer* **11:** 338–351

Rulifson EJ, Blair SS (1995) Notch regulates wingless expression and is not required for reception of the paracrine wingless signal during wing margin neurogenesis in Drosophila. *Development* **121:** 2813–2824

Sharma VM, Calvo JA, Draheim KM, Cunningham LA, Hermance N, Beverly L, Krishnamoorthy V, Bhasin M, Capobianco AJ, Kelliher MA (2006) Notch1 contributes to mouse T-cell leukemia by directly inducing the expression of c-myc. *Mol Cell Biol* **26:** 8022–8031

Simmonds AJ, Liu X, Soanes KH, Krause HM, Irvine KD, Bell JB (1998) Molecular interactions between Vestigial and Scalloped promote wing formation in Drosophila. *Genes Dev* **12:** 3815–3820

Wang H, Zou J, Zhao B, Johannsen E, Ashworth T, Wong H, Pear WS, Schug J, Blacklow SC, Arnett KL, Bernstein BE, Kieff E, Aster JC (2011) Genome-wide analysis reveals conserved and divergent features of Notch1/RBPJ binding in human and murine T-lymphoblastic leukemia cells. *Proc Natl Acad Sci USA* **108:** 14908–14913

Weng AP, Millholland JM, Yashiro-Ohtani Y, Arcangeli ML, Lau A, Wai C, Del Bianco C, Rodriguez CG, Sai H, Tobias J, Li Y, Wolfe MS, Shachaf C, Felsher D, Blacklow SC, Pear WS, Aster JC (2006) c-Myc is an important direct target of Notch1 in T-cell acute lymphoblastic leukemia/lymphoma. *Genes Dev* **20:** 2096–2109

Williams JA, Paddock SW, Carroll SB (1993) Pattern formation in a secondary field: a hierarchy of regulatory genes subdivides the developing Drosophila wing disc into discrete subregions. *Development* **117:** 571–584

Wu S, Liu Y, Zheng Y, Dong J, Pan D (2008) The TEAD/TEF family protein Scalloped mediates transcriptional output of the Hippo growth-regulatory pathway. *Dev Cell* **14:** 388–398

Yan S-J, Gu Y, Li WX, Fleming RJ (2004) Multiple signaling pathways and a selector protein sequentially regulate Drosophila wing development. *Development* **131:** 285–298

Zecca M, Struhl G (2007) Control of Drosophila wing growth by the vestigial quadrant enhancer. *Development* **134:** 3011–3020